Published in final edited form as:
J Immunol. 2015 February 1; 194(3): 1047–1056. doi:10.4049/jimmunol.1401832.

CD40L induces functional tunneling nanotube networks exclusively in dendritic cells programmed by mediators of type-1 immunity

Colleen R. Zaccard[*], **Simon C. Watkins**[†], **Pawel Kalinski**[*,‡,§,¶], **Ronald J. Fecek**[*], **Aarika L. Yates**[*], **Russell D. Salter**[§], **Velpandi Ayyavoo**[*], **Charles R. Rinaldo**[*,||,#], and **Robbie B. Mailliard**[*,**,#]

[*]Department of Infectious Diseases and Microbiology, University of Pittsburgh, Pittsburgh, PA, 15261 U.S.A

[†]Department of Cell Biology and Physiology, University of Pittsburgh, Pittsburgh, PA, 15261 U.S.A

[‡]Department of Surgery, University of Pittsburgh, Pittsburgh, PA, 15261 U.S.A

[§]Department of Immunology, University of Pittsburgh, Pittsburgh, PA, 15261 U.S.A

[¶]Department of Bioengineering, University of Pittsburgh, Pittsburgh, PA, 15261 U.S.A

[||]Department of Pathology, University of Pittsburgh, Pittsburgh, PA, 15261 U.S.A

Abstract

The ability of dendritic cells (DC) to mediate $CD4^+$ T cell help for cellular immunity is guided by instructive signals received during DC maturation, and the resulting pattern of DC responsiveness to the Th signal, CD40L. Furthermore, the professional transfer of antigenic information from migratory DC to lymph node-residing DC is critical for the effective induction of cellular immune responses. Here we report that, in addition to their enhanced IL-12p70 producing capacity, human DC matured in the presence of inflammatory mediators of type-1 immunity (DC1) are uniquely programmed to form networks of tunneling nanotube-like structures in response to CD40L-expressing Th cells or recombinant CD40L. This immunologic process of DC 'reticulation' facilitates intercellular trafficking of endosome-associated vesicles and Ag, but also pathogens such HIV-1, and is regulated by the opposing roles of IFN-γ and IL-4. The initiation of DC reticulation represents a novel helper function of CD40L and a superior mechanism of intercellular communication possessed by DC1, as well as a target for exploitation by pathogens to enhance direct cell-to-cell spread.

Introduction

Dendritic cells (DC) play a central role in the initiation and regulation of the immune response. They bridge the innate and adaptive branches of immunity by gathering pathogen-

[**]Corresponding author: Phone: 412-624-3848 Fax: 412-383-8926 rbm19@pitt.edu.
[#]Co-senior author,

and tissue-derived environmental cues and translating this information into the development of appropriate adaptive immune responses following their migration to draining lymph nodes (1). The combination of exogenous and endogenous activation signals received in the affected tissue during their immature stage results in their differentiation into mature, pre-programmed DC capable of inducing differentially polarized, Ag-specific immune responses (2, 3).

The ability of DC to drive the appropriate type of adaptive immune response to effectively counter a particular pathogen assault is greatly influenced by their interaction with $CD4^+$ Th cells and their responsiveness to Th cell-associated CD40L, a critical factor in 'licensing' or enabling DC to promote cellular immunity (4–6). Type-1 polarized DC (DC1) (2), or DC matured under pro-inflammatory conditions by immune mediators typically associated with acute viral infections, such as viral RNA (3), type-1 IFN (7), and activated NK cells (8), respond to CD40L by producing enhanced levels of IL-12p70, a key driving factor of Th1-biased cellular immunity (9). Conversely, 'standard' or type-2 polarized DC (DC2) (2), such as those matured in the presence of histamines or prostaglandin E_2 (PGE_2) (3, 10), drive Th2-biased responses, display a diminished capacity to produce IL-12p70 upon CD40 ligation, and are less effective at driving cell-mediated immunity.

DC migration and transportation of Ag to draining lymph nodes are critical for the initiation of CTL responses (1). This process also involves immune communication with a subset of lymph node resident DC that possess an enhanced ability to cross-present Ag to $CD8^+$ T cells (11, 12). Transfer of antigenic information between migratory and lymph node residing DC has been shown to be essential in models of immunity to viruses (12, 13), but the exact mechanisms involved in this Ag exchange are unclear. In situ imaging studies have revealed that migratory DC undergo dramatic morphological alterations upon entry into lymph nodes, including the formation of extended membrane processes, as they are integrated into a network of lymphoid residing DC (14), thus supporting the concept of direct Ag transfer. One proposed mode of direct intercellular Ag exchange occurs through the facilitation of tunneling nanotubes (TNTs), or thin F-actin-based membrane protrusions that form direct cytoplasmic connections between proximal and remote cells (15, 16). TNTs can support the intercellular transfer of organelles, cytoplasmic and cell surface proteins, calcium fluxes, as well as some pathogens (16). While TNTs and their function in the transmission of signaling fluxes have been described in immature DC (iDC) (17), little information exists concerning the nature of their induction in mature DC, their function in DC-mediated communication, or their role in innate and adaptive immunity.

Here we describe a novel immunologic process by which networks of TNTs are induced as an exclusive trait of mature, high IL-12-producing DC1 in response to the Th cell activation signal, CD40L. We show that these CD40L-induced structures indeed support the direct intercellular transfer of cytoplasmic and cell surface-associated material between DC. Moreover, this novel process of DC 'reticulation' dramatically increases cell surface area and spatial reach, thus enhancing the likelihood of their contact with Ag-specific T cells and other DC. Importantly, the ability of DC to reticulate in response to CD40L is imprinted during maturation by exposure to type-1 inflammatory mediators, which are typically present during acute viral infection. While the induction of reticulation represents a novel

helper function of $CD4^+$ T cells that serves to facilitate efficient DC1-mediated intercellular communication, this immune process can also be exploited by pathogens such as HIV-1 for direct cell-to-cell spread.

Materials and Methods

Isolation of human primary cells

Whole blood products (buffy coats) from healthy, anonymous donors were purchased from the Central Blood Bank of Pittsburgh. Autologous $CD14^+$ monocytes, $CD3^+$ T cells, $CD4^+$ T cells, $CD8^+$ T cells, and myeloid blood-derived DC were isolated from PBMC by density gradient separation (18) followed by immunomagnetic negative selection of the respective cell types (EasySep: STEMCELL Technologies Inc., Vancouver, BC, Canada).

Generation of DC

Monocytes were cultured for 5–7 d at 37°C in IMDM (Gibco, Life Technologies, Grand Island, NY) supplemented with 10% fetal bovine serum (cIMDM) in the presence of GM-CSF and IL-4 (both 1000 IU/ml; R&D Systems, Minneapolis, MN). DC generated under serum free conditions using either AIM-V (Gibco) or Cellgenix base media were also tested and yielded similar results (data not shown). On d 5, iDC were differentially exposed to activation factors for 48 h. For mature DC1, the activation factors consisting of combinations of either polyisosinic:polycytidylic acid [poly(I:C)] (20 μg/ml), IFN-α (3,000 units/ml), TNF-α (50 ng/ml), IL-1β (25 ng/ml), and IFN-γ (1,000 IU/ml) (7), LPS (250 ng/ml) and IFN-γ (1,000 IU/ml), or R848 (2.5 μg/ml) (Enzo Life Sciences, Farmingdale, NY) and IFN-γ (1000 IU/ml). Alternatively, DC1 were generated by co-culturing iDC with IL-18-primed NK cells in the presence of IL-15 (1 ng/ml) (8), or $CD8^+$ T cells in the presence of staphylococcal enterotoxin B (SEB) (1 ng/ml) (19) (Sigma-Aldrich, Saint Louis, MO). Mature, low IL-12p70 producing DC2 were generated using a modified version of a previously described cocktail consisting of TNF-α (50 ng/ml), IL-1β (25 ng/ml), and PGE_2, (10^{-6} mol/L) (7), a combination of LPS (250 ng/ml) and PGE_2 (10^{-6} mol/L) (10), or R848 (2.5 μg/ml) and PGE_2 (10^{-6} mol/L). Monocyte-derived DC0 were generated by exposure to TNF-α, LPS, or R848 alone for 24 h (10, 19). Similarly, freshly isolated blood-derived myeloid DC were treated for 24 h with TNF-α prior to secondary stimulation.

CD40L-induced activation of mature DC

Differentially matured DC were stimulated for 24 h with either recombinant human (rh)CD40L (0.5 μg/ml) (MegaCD40L; Enzo Life Sciences) or CD40L-expressing J558 (J558-CD40L) cells (Dr. P Lane, University of Birmingham, United Kingdom) (10), which were added to DC cultures at a 1:1 ratio. Where specified, IL-4 (5000 IU/ml), IL-10 (0.1 μg/ml), or IFN-γ (5000 IU/ml) was also included during CD40L stimulation.

IL-12p70 production and screening

DC were harvested, washed, and plated in 96 well flat bottom plates (3×10^5 cells/well), and stimulated with either J558-CD40L cells or rhCD40L. IL-12p70 was measured in 24 h supernatants using the MSD electrochemiluminescence detection system (MesoScale Discovery, Rockville, MD).

DC-T cell co-cultures

Differentially matured DC (1.25×10^5 cells/ml) were co-cultured with $CD4^+$ or $CD8^+$ T cells (3.75×10^5) cells/ml in the presence of absence of SEB (1μg/ml). When used, CD40L blocking mAb (Enzo Life Sciences) or control mAb (BD Biosciences, San Jose, CA) were added to the cultures. Bright field microscopic images (400×) were collected from 5–10 randomly selected fields in independent experiments from 3 healthy donors.

Flow cytometry

The following immunostaining Ab reagents were used for flow cytometry analysis: Mouse-anti-human CD83-PE, CD86-PE, OX40L-PE, CD40L-PE, CD3-FITC, CD4-APC, CD8-APC, CD19-PE, CD3-PE, HLA-DR-FITC (all from BD Biosciences), CD40-PE, CD56-PE (Beckman Coulter, Indianapolis IN U.S.A.), CCR7-FITC (R&D Systems), CD14-PE, CD1c-PE (Miltenyi Biotech, San Diego, CA) and the respective matched isotype controls (BD Biosciences). Prior to analysis for expression of CD40L, isolated $CD4^+$ and $CD8^+$ T cells were stimulated for 24 h with anti-CD3/CD28 activating Dynabeads (Gibco, Life Technologies). Purity was determined by the exclusive expression of either CD4 or CD8 on the $CD3^+$ gated lymphocytes. Purity of blood-isolated DC was delineated using the following gating strategy: lineage $(CD3, CD14, CD19, CD56)^-$ and $CD1c^+$ $HLA\text{-}DR^+$. Analysis was performed using the BD Biosciences LSR Fortessa Cell Analyzer and FlowJo version 7.6 software.

Immunocytochemistry

DC1 were transferred to chambered borosilicate cover-glass slides (Lab-Tek, Thermo Fisher Scientific, Rochester, NY) and treated with rhCD40L or media for 18–20 h prior to processing. Samples were fixed and permeabilized with 0.1% Triton X-100 and non-specific mAb binding blocked with 2% BSA. Primary mouse anti-human early endosomal Ag 1 (EEA1) or isotype control mAb (1.25 μg/ml) (BD Transduction Laboratories, San Jose, CA) were added, followed by secondary goat-anti-mouse Alexa-Fluor 488-conjugated mAb and rhodamine-conjugated phalloidin (Molecular Probes, Invitrogen, Eugene, OR) to label primary mAb and filamentous F-actin, respectively. Nuclei were stained with Hoeschst stain (Invitrogen, Life Technologies).

Microscopy

Live-cell differential interference contrast (DIC) and confocal images were collected using a Nikon Eclipse Ti and Photometrics Evolve camera system with a Nikon Apo TIRF 60× Oil DIC N2 objective lens with a numerical aperture (NA) of 1.49; and NIS-Elements software was used to collect and analyze data. Additionally, images of fixed cells were collected on the Olympus Fluoview 1000 microscope system with Olympus 60× objective lens (NA=1.4). Standard bright field images were collected using a Leica DM IL LED using a Leica HI Plan I Ph2 40× objective lens (NA=0.5) using a Leica EC3 Camera system, and images were analyzed using Leica Application Suite software. Live cell cultures were maintained in an imaging chamber at 37°C and 5% CO_2 in media (cIMDM) during image acquisition, while fixed cells were maintained in PBS.

Morphological analysis of DC by high resolution imaging

DC (1.25×10^5 cells/ml) were cultured in glass-bottomed microwell imaging dishes (MatTek Corporation, Ashland, MA). Time-lapse live-cell DIC imaging was captured at time points and durations specified, with illumination intervals ranging from 2 to 6 min. For confocal imaging experiments, DC were either maintained in media alone (resting) or exposed to rhCD40L for 18 to 20 h, followed by surface staining using anti-human HLA ABC:Alexa Fluor 488 Ab (AbD Serotec, Raleigh, NC) as previously described (17, 20), and cell nuclei were stained with HCS Nuclear Mask Red Stain (Invitrogen, Life Technologies). To quantitate total cell surface area and membrane morphologies, the cytoplasm was additionally stained with 0.39 μg/ml (0.4 μM) CFSE (Molecular Probes, Invitrogen), and IMARIS imaging software (Bitplane, South Windsor, CT) was used for data analysis.

Peptide and protein Ags

The following Ag sources were used at the concentrations listed in the described Ag transfer experiments: 0.2 μg/ml of CMV Ag (a pool of 9- to 12-mer peptides that comprise the CMV portion of the common control CMV, EBV, and influenza A virus peptide pool (21)); 0.4 μg/ml of varicella zoster virus (VZV) Ag (18mer overlapping peptide pool spanning the entire glycoprotein E; Sigma-Aldrich); and 0.5 μg/ml of tetanus toxoid (TT) Ag (whole protein; Astarte Biologics, Bellevue, WA).

Intercellular bead and Ag transfer experiments

'Donor' DC1 and DC2 were generated by pulsing iDC with 40 nm yellow-green (YG) latex nano-beads (Molecular Probes, Invitrogen) at 1×10^{10} beads/ml and exposed them to the respective polarizing cocktails. For Ag transfer experiments, CMV, VZV, and TT Ags were added along with the beads and again after 24 h. Donor DC containing beads and 'recipient' DC lacking beads were labeled with cyanine dyes (Cy)5 or Cy3 dye (GE Health Care, Piscataway, NJ U.S.A.), respectively, for 20 min at room temperature. Donor and recipient DC1 or DC2 were harvested, washed 5 times, and co-cultured for 20 h in the presence or absence of rhCD40L. Where stated, a 0.45 μm trans-well system (Corning Costar, Tewksbury, MA) was used to separate co-cultured DC. Bead transfer to recipient DC was assessed by flow cytometry, as well as by live-cell confocal microscopy.

For Ag transfer experiments, donor DC1 were co-cultured with Cy5-labeled recipient DC1 for 20 h in the presence of rhCD40L. Cy5-labeled recipient DC1 were then differentially sorted based on YG bead expression (as a marker for donor to recipient DC1 intercellular exchange) using a BD FACS Aria IIu cell sorter. Sorted YG^+ (bead-containing) and YG^- (bead-deficient) recipient DC1 were used as Ag-presenting stimulators of autologous T cell responses in a modified version of a previously described extended in vitro sensitization and IFN-γ ELISPOT assay (22). Briefly, the sorted DC1 and autologous $CD3^+$ T cells were co-cultured for 10 d at a DC:T cell ratio of 1:10, with rIL-2 (100 IU/ml; Novartis, New York, NY) added on d 3. The cultured T cells (3×10^4/well) were tested by ELISPOT for reactivity to the individual CMV, VZV, and TT Ags in the presence of autologous monocytes (5×10^4/well). Spots were counted using an automated ELISPOT reader (AID), and expressed as mean Ag specific IFN-γ spot forming units (SFU) per 10^5 cells, subtracting values from Ag negative control wells.

Detection of intercellular trafficking of pathogens

Bacteria transfer studies—DC1 were cultured in imaging dishes and stimulated with CD40L for 8–10 h, prior to placement into the imaging chamber, which was maintained at 37°C and 5% CO_2. Live EGFP-expressing bacteria (*Escherichia coli* strain BL21DE3) suspensions were prepared by picking a green isolated colony, and suspending it in 200 μl cIMDM. Ten μl of the *E. coli* mix was then injected into the media directly above cells. Cultures were incubated for 2 h to allow bacteria to settle in the proximity of the DC monolayer, and sequential images were generated using confocal resonance scanning methods.

Virus-like particle transfer studies—HIV-1-like particles were generated by transfecting 293T cells with pGag-EGFP, pRev, pGag/Pol, and pHXB2-Env using polyjet reagent (SignaGen Laboratories, Gaithersburg, MD) per manufacturer's instructions. Seventy-two h post-transfection, supernatants were collected, spun at 3000 rpm for 10 min and filtered through a 0.22 μm filter to remove cellular debris. Particles were concentrated by ultracentrifugation and resuspended in PBS. Virus titer was quantitated by p24 ELISA. Cy5-labeled donor DC1 were pulsed with 26.2 ng/ml HIV-1-like particles for 1 h and then washed extensively to remove unbound particles. Recipient DC1 were labeled with Cy3 and co-cultured in imaging dishes with donor DC1 the presence of CD40L for 8–12 h or 18–22 h prior to live-cell, time-lapse confocal imaging.

Statistics

Quantitative IMARIS data were analyzed using a two way ANOVA or unpaired student t test (with Welch's correction for unequal SD, when necessary), and significance determined at α of 0.05. Data are represented as mean ± SD of 3 healthy donors. For experimental data generated by exposing DC types to CD40L ± IL-4, IL-10, or IFN-γ, the percentage of reticulation positive cells ± SE is from 1 representative of 3 donors tested (>50 cells assessed/condition), and statistical significance was determined using Fisher's exact test. YG^+ versus YG^- recipient DC conditions in the Ag transfer studies reflect 2 independent experiments that are represented as mean ± SE; statistical comparisons were performed using unpaired student t tests.

Results

CD40L-expressing $CD4^+$ T cells induce the formation of TNT-like extensions in DC1 matured by acute inflammatory factors or activated immune effector cells

Autologous monocyte-derived human DC were used as Ag presenting cells to stimulate $CD4^+$ and $CD8^+$ T cell subsets to study the in vitro T cell activation potential of differentially polarized mature DC. Our method for generating mature DC1 utilized the previously described αDC1 cocktail, consisting of poly(I:C), TNF-α, IL-1β, IFN-α, and IFN-γ (7). These DC1 were characterized by expression of CD83, $CD86^{high}$, and CCR7, and their enhanced IL-12p70 production capacity when subsequently exposed to CD40L (Supplemental Fig. 1A). In contrast, DC2 were generated using a previously described cytokine cocktail consisting of IL-1β, TNF-α, IL-6 and PGE_2 (10), and characterized by their surface expression of CD83, $CD86^{high}$, CCR7, and OX40L, and their diminished

capacity to produce IL-12p70 (Supplemental Fig. 1A). Using standard bright field microscopy, we observed that DC1, but not DC2, developed TNT-like membrane extensions when co-cultured for 24 h with $CD4^+$ T cells in the presence of the Ag surrogate, SEB (Fig. 1A). Importantly, the formation of these membrane bridges required the presence of Ag as well as $CD4^+$ T cells, and did not occur in co-cultures containing $CD8^+$ T cells (data not shown).

We next sought to determine why these morphological changes were unique to DC1 co-cultured with $CD4^+$ T cells, but not $CD8^+$ T cells. We investigated the role of the DC-activating molecule CD40L in our system since its expression is rapidly induced on $CD4^+$ T cells, but not $CD8^+$ T cells, upon Ag-specific activation (7), as demonstrated by their stimulation with anti-CD3/CD28 activating beads (Supplemental Fig. 1B, left). Moreover, both DC1 and DC2 comparably expressed the ligand's receptor CD40 (Supplemental Fig. 1B, right). To test whether this effect on DC1 was CD40L-dependent and could occur independently from other T cell-derived factors, we exposed the differentially activated DC to either a J558-CD40L cell line or the control CD40L-deficient J558 cells. When stimulated with the J558-CD40L cells, DC1 developed membrane protrusions similar to those induced by the $CD4^+$ T cells (Supplemental Fig. 1C). However, this did not occur with exposure to the CD40L-negative J558 control cells (Supplemental Fig. 1C); and once again, DC2 failed to develop these formations (data not shown). We also tested the direct effect of adding rhCD40L to DC types (Fig. 1A), which induced a similar network of TNT-like membrane processes in DC1, but not DC2, in up to 25 donors tested. When CD40L-blocking mAb was added to 24 h DC1-$CD4^+$ T cell co-cultures, the formation of the membrane extensions was inhibited (Fig. 1B). Together, these data definitively show that the Th cell factor CD40L is an inducer of the described morphological alterations occurring exclusively in DC1.

Live-cell confocal fluorescence microscopy revealed that DC1 develop extensive networks of TNT-like processes in response to CD40 ligation (Fig. 1C), and we used IMARIS 3D imaging analysis software to quantitate the morphological changes observed in the DC types (Fig. 1D). This evaluation showed that the total cell surface area dramatically increased in CD40L-activated DC1 compared to resting DC1, and to a lesser degree in DC2 upon activation (Fig. 1E). Importantly, a significant difference in surface area was shown between DC1 and DC2 following rhCD40L treatment (Fig. 1E). In their resting state, we found that 27.2% of DC1 already displayed ≥5 long, ultrafine, non-branching TNTs similar to those previously described in iDC (17), while only 2.4% of resting DC2 displayed multiple TNTs (Fig. 1F). CD40L-activated DC1 displayed a substantial increase in TNT-like extensions, which varied widely in length, diameter, and complexity, established multiple linkages between neighboring cells, and were occasionally detected above the substratum (Video 1). In contrast, the CD40L-activated DC2 were typically smaller and more rounded than DC1, and displayed membrane ruffling as opposed to TNT-like extensions (Video 2). For analysis of the more complex membrane formations, we characterized each 'filament' (Fig. 1D, middle panel), defined as a group of connected dendrite- and TNT-like segments that branched from a single origin point at the edge of the cell body. The analysis showed that 100% of CD40L-activated DC1 displayed a reticulate membrane morphology (≥5 filaments per cell), compared to 16.7% of CD40L-activated DC2 (Fig. 1G). Among the reticulation positive cells, filaments expressed by DC2 tended to be lesser in number, shorter in length,

and displayed less complexity of branching than that of DC1 (Supplemental Fig. 1D–1G). Furthermore, CD40L-induced membrane extensions dramatically extended the spatial reach of DC1 compared to DC2 (Fig. 1H), as determined by measuring the shortest distance from the origin point to the distal terminal point of each filament (Fig. 1D, right panel).

We were curious whether the CD40L-induced reticulation process was related to the particular cocktail(s) of activation factors used in our initial experiments, or if this was in fact a general characteristic of DC1. While a variety of pathogen- or host-derived signals can induce DC maturation, the presence of either IFN-γ or PGE_2 during the maturation process is particularly important for driving differential DC polarization (2, 8, 10, 19, 23). To further explore the role of these key polarization factors in priming DC for reticulation, we tested the CD40L effect using alternative methods for generating DC0, DC1, and DC2 from iDC precursors utilizing different TLR agonists, such as LPS (TLR4) or R848 (TLR7/8) alone, or in combination with IFN-γ or PGE_2, respectively (10, 24, 25). DC1 generated using these alternative methods formed extensive TNT networks in response to secondary CD40L activation, while DC2 failed to do so, and non-polarized DC0 displayed an intermediate morphology (Fig. 2A, 2B). Additionally, we tested other previously published cellular methods to induce DC1, using either activated NK cells (8) or Ag-stimulated $CD8^+$ T cells (19, 26). As was found with the other DC1 types, both NK cell- as well as $CD8^+$ T cell-induced DC1 responded to secondary CD40L stimulation by forming networks of TNTs (Fig. 2C). Together, these data highlight that reticulation is indeed a characteristic trait of DC matured under type-1 inflammatory conditions, while PGE_2-exposed DC2 are refractory to the reticulation process.

Opposing roles of IFN-γ and IL-4 in regulating the CD40L-induced DC reticulation process

Pre-programmed DC1 can be generated from iDC by treatment with maturation factor(s) in combination with IFN-γ, but concomitant activation of a mature non-polarized DC0 with IFN-γ and CD40L can also induce high IL-12 production, similar to that of DC1 treated with CD40L alone (18, 19). We speculated that IFN-γ might also act in an analogous fashion, along with CD40L, as a co-stimulator of the reticulation process in DC0. Therefore, we tested the co-stimulatory effect of this Th1-associated cytokine, as well as the respective Th2- and regulatory T cell-associated cytokines, IL-4 and IL-10 (3), on reticulation in TNF-α-matured DC0. We found that, in addition to augmented IL-12p70 production (data not shown), IFN-γ co-stimulation enhanced the ability of DC0 to reticulate in response to CD40L (Fig. 3A). Intriguingly, co-exposure of DC0 to CD40L and IL-4 substantially reduced the percentage of reticulation positive cells, while IL-10 had no significant impact on reticulation (Fig. 3A). We next investigated the effect of these differential Th cell-associated cytokines on CD40L-induced reticulation in pre-programmed DC1, and revealed an even more substantial inhibitory effect of IL-4 on this process (Fig. 3B). Again, the addition of IL-10 had no significant impact on the ability of DC1 to reticulate.

The method of generating DC from monocytes in vitro allows for sufficient cell numbers to be obtained for research studies and clinical applications (1), and represents an established model for migratory DC that arise in vivo from the differentiation of monocyte precursors (13, 27). Nevertheless, we were interested to see if DC isolated directly from human

peripheral blood could be induced to form TNT networks by CD40L in an IFN-γ-dependent manner, analogous to the behavior of monocyte-derived DC. $CD1c^+$ $HLA\text{-}DR^+$ myeloid DC were isolated from fresh PBMC by magnetic bead enrichment and matured with TNF-α for 24 h prior to treatment with media, rhCD40L, or IFN-γ + rhCD40L, followed by live-cell confocal imaging. Although low cell numbers limited the scope of these experiments, we established that concomitant exposure of TNF-α-matured, myeloid DC to the Th1 cytokine IFN-γ enhanced the formation of networks of ultrafine TNTs in response to CD40L (Supplemental Fig. 2). TNTs observed in peripheral blood DC tended to be thin and non-branching, as opposed to the complex structures observed in monocyte-derived DC, but these structures established multiple intercellular connections and were frequently detected above the substratum (data not shown), similar to those observed in monocyte-derived DC1.

CD40L-induced reticulation supports the direct transfer of cellular contents between DC1

TNTs described in the current literature establish both membrane and cytoplasm continuity between connected cells, which in turn provides a pathway for direct intercellular communication (16). Indeed, TNTs can facilitate the direct exchange of organelles and both cytoplasmic and membrane-associated components (16, 28). We therefore speculated that the reticulation process could allow for efficient transfer of cellular contents between proximal and remote DC1. We first used high resolution DIC imaging to capture the formation of the TNT-like networks over time, and to search for visual evidence of the trafficking of cellular content between live DC via CD40L-induced TNTs. In doing so, we were able to clearly observe the dynamic immune process of reticulation, whereby DC actively formed numerous membrane extensions within hours of exposure to rhCD40L, ultimately establishing a network of interconnected processes between proximal and remote DC (Fig. 4A; Video 3). Moreover, a number of endogenous vesicles could be seen traveling rapidly from one cell to another through these structures (Fig. 4B; Video 4). We hypothesized that the membrane conduits were facilitating direct DC-to-DC transfer of endosomal vesicles, as has been shown in other cell types (15, 29). To address this, we fixed CD40L-stimulated DC1 and stained them with EEA1 mAb and Rh-Phalloidin for labeling endosomes and F-actin-based TNTs, respectively. We were able to clearly detect early endosome localization within CD40L-induced TNTs (Fig. 4C) by confocal microscopy, despite the disruption of the majority of fine membrane extensions by the fixation and staining process. These data indicate that DC1 can utilize the process of reticulation to exchange endosome-associated vesicles between interconnected cells.

In order to test if exogenous material could also be acquired and subsequently exchanged between DC1 by the same mechanism, we pulsed iDC with YG-labeled nano-beads representing Ag, and then differentially matured them to achieve their DC1 or DC2 status. We labeled bead-containing ‘donor’ DC and bead deficient ‘recipient’ DC with Cy5 and Cy3, respectively, and co-cultured the DC for 20 h in the presence or absence of rhCD40L. Using time-lapse confocal imaging of live cells, beads were observed to localize to the TNTs of donor DC1, and rapidly traverse the length of these structures (Fig. 5A; Video 5). Furthermore, the pathway of individual beads could be traced as they traveled through blue donor DC1 membrane extensions into the recipient cell, where they finally collected in the cell body (Fig. 5B).

In parallel to, and in support of the live-cell imagine studies, bead transfer was quantified by flow cytometry, as determined by detection of fluorescent beads in Cy3-labeled recipient cells in overnight resting or activated co-cultures. Using this method, we demonstrated that the transfer of labeled beads from donor to recipient DC was enhanced in CD40L-activated DC1 compared to resting DC1, as well as resting and activated DC2 (Fig. 5C). Moreover, while a small fraction of DC2 recipients in the CD40L-activated conditions acquired beads, the mean fluorescence intensity of the bead-containing DC1 recipients was nearly 4 fold greater than that of the DC2 recipients (Fig. 5C), indicating a higher number of beads transferred to recipient DC1 on a per cell basis. We next evaluated the ability of recipient DC1 to functionally utilize and present Ags acquired from donor DC1 following reticulation. Briefly, we pulsed iDC with a combination of CMV, VZV, and TT Ags in addition to YG nano-beads during their exposure to type-1 polarizing maturation factors to generate Ag- and bead-loaded donor DC1. These donor DC1 were co-cultured with Cy5-labeled recipient DC1 in the presence of rhCD40L for 20 h. Using the YG beads from donor DC1 as a marker for CD40L-induced intercellular exchange, two distinct populations of recipient DC1 (YG^+ and YG^-) were isolated by FACS sorting. The sorted YG^+ and YG^- recipient DC1 were assessed for their differential capacity to drive Ag-specific recall responses in autologous T cell using an established 10 d in vitro sensitization assay followed by an IFN-γ ELISPOT readout. Sorted YG^+ transfer recipient DC1 displayed an enhanced ability to drive Ag-specific T cell responses compared to YG^- DC1 (Fig. 5D). Conversely, recipient DC1 separated from reticulating donor DC1 using a trans-well system in parallel co-cultures failed to generate substantial Ag-specific T cell responses (Supplemental Fig. 3), indicating that the functional transfer of Ag during the reticulation process was contact dependent.

The DC reticulation process facilitates intercellular trafficking of microbial pathogens

While the CD40L-mediated induction of TNT networks could play an important role in intercellular communication or Ag transfer between interconnected DC, current literature suggests that bacterial (29) as well as viral pathogens such as HIV-1 (16, 30, 31) can exploit TNTs for direct cell-to-cell transmission. We hypothesized that CD40L-induced reticulation in DC1 could similarly provide an efficient pathway for intercellular trafficking of microbes.

In order to determine if direct cell-to-cell bacterial transfer can occur via CD40L-induced TNT networks, we first injected a suspension of live EGFP-expressing *Escherichia coli* into DC1 cultures following their 10 h stimulation with rhCD40L. Time-lapse confocal resonance scanning was conducted 2 h later to capture the trafficking of live bacteria between DC1. Similar to what has been described in macrophages (29), this experimental strategy clearly revealed bacteria rapidly ‘surfing’ along the outside of TNT-like membrane bridges from one cell to another (Fig. 6A; Video 6). Notably, individual bacterium could simultaneously travel in opposite directions along the same tube, as well as change directions in mid-transfer. CD40L-induced extensions could also be seen to capture bacteria and draw them toward the cell body for subsequent internalization (data not shown). These data reveal a mechanism by which CD40L-activated DC can use TNT-like extensions to probe for pathogens in tissues, or a pathway by which bacteria can spread from cell-to-cell over long distances, potentially facilitating their dissemination.

To confirm that DC reticulation could also support intercellular trafficking of viral pathogens, we pulsed Cy5-labeled DC1 with EGFP-expressing HIV-1-like particles and co-cultured these donor DC with Cy3-labeled recipient DC1. The DC co-cultures were then stimulated with rhCD40L for either 10 or 20 h prior to live-cell confocal microscopy. Maximum intensity projection images revealed particle localization to TNTs of the reticulating donor cells that connected with recipient cell bodies at both 10 h (Fig. 6B) and 20 h time points (Fig. 6C). Furthermore, HIV-1-like particles were frequently detected at the interface between donor cell TNTs and recipients, prior to their transfer to recipient cell bodies, up to 24 h after the donor DC first acquired the particles (Fig. 6C). Together, these findings demonstrate that the induction of DC reticulation by CD40L can facilitate rapid and direct spread of pathogens such as bacteria or HIV-1 between interconnected immune cells.

Discussion

We describe in this report the induction of the immune process of ‘reticulation’, a novel aspect of CD40L-mediated $CD4^+$ T cell help that results in the formation of dynamic networks of TNT-like membrane extensions between proximal and remote DC. We determined that the ability of human myeloid DC to reticulate is imprinted by specific combinations of pathogen- and host-derived inflammatory signals that they receive during maturation. Importantly, migratory, high IL-12p70-producing DC1 appear to be ‘licensed’ to reticulate in response to CD40 ligation, while DC2 are refractory to this process.

Current research suggests a multifarious role for TNTs in intercellular communication, but their mode of induction and function in the context of DC-mediated immunity has not been fully elucidated. Studies using iDC have demonstrated that TNTs induced by mechanical stimulation or *Escherichia coli* supernatants support cell-to-cell propagation of calcium fluxes, which are integral to the regulation of DC activation (17). A recent investigation showed that MHC class II^+ DC in mouse corneas form TNTs in response to trauma or LPS activation, highlighting a potential link between inflammation and TNT formation for the first time in vivo (32). We showed that DC matured under type-1 inflammatory conditions display an enhanced number of unbranched ultrafine TNTs compared to DC2 in their resting state prior to in secondary activation. However, the distinctive responsiveness of pre-programmed DC1 to secondary CD40L stimulation, or DC0 to concomitant CD40L and IFN-γ stimulation, results in the formation of a far more extensive and complex network of TNTs. Although CD40L-induced TNTs appear to be most similar to those described in macrophages due to their heterogeneous structure (29), they typically exhibit a unique branching pattern that results in a highly complex, interconnected web of DC.

Since the initial description of TNTs by Rustom *et al.* (15) in 2004, TNTs have been shown to facilitate the direct transfer of cytosolic and membrane components, such as endosome- and lysosome-associated vesicles and MHC molecules (16, 28). Previous in vivo studies have also shown that non-migratory lymph node-residing DC specializing in cross-presentation acquire Ag and Ag-loaded MHC molecules from migratory DC for the efficient induction of CTL responses (12, 13). While Ag acquisition by DC has been demonstrated through a number of alternate mechanisms (33–35), we demonstrate that the reticulation process can facilitate intercellular Ag exchange for the enhancement of Ag-specific T cell

responses, and we propose that this represents an additional novel mechanism by which the acquisition occurs in vivo.

Recent in situ imaging advances have provided evidence of dynamic DC membrane extensions forming intercellular networks in lymph nodes or facilitating probing for microbial pathogens in non-lymphoid tissues. In lymph nodes, resident DC are positionally fixed in a distributed manner along a complex fibroblastic reticular network, which defines the T cell zones and guides T cell migration and scanning of DC (36). These DC are linked by the tips of extended membrane processes, which also facilitate rapid and pervasive probing (37). Migratory DC that travel to the T cell areas of regional lymph nodes undergo frequent changes in morphology, including the formation of dendrite-like extensions (14, 37), and become sessile within 2 d as they are likely integrated into the resident DC network (37). These studies collectively provide in vivo evidence of a meshwork of DC fixed on the fibroblastic reticular network of lymph nodes. Our study demonstrates the unique ability of Th cells to regulate the formation of intercellular TNT networks in differentially polarized DC, yet the exact contribution of CD40L-induced reticulation to migratory and resident DC interactions in vivo remains to be determined. In addition to DC dynamics in nodes, this process may also assist pathogen acquisition by sentinel DC in mucosal tissues. Interestingly, intravital imaging of the lamina propria has revealed an increase in dynamic trans-epithelial DC extensions upon introduction of enteric bacterial pathogens (38). We have shown that, in addition to type-1 inflammatory mediators, DC exposed to signals from pathogens develop TNTs, and speculate that contact with CD40L-expressing effector Th cells could further enhance the number of pathogen-probing extensions formed by DC in the mucosa.

While DC reticulation is likely important for direct communication between immune cells, this process may conversely facilitate progression of chronic diseases such HIV-1 or cancer. The bidirectional transfer of vesicles, proteins, and mitochondria via TNTs has been recently observed between malignant human pleural mesothelioma cells and lung adenocarcinoma tumor specimens (39), suggesting a detrimental role for TNTs in cancer. Similarly, TNTs can be hijacked by intracellular pathogens to enhance rapid spread to distant cells, while avoiding the inhospitable extracellular milieu. HIV-1 was shown to induce TNTs in infected macrophages and utilize them for high-speed transmission to neighboring uninfected macrophages (30, 31). Interestingly, HIV-1 infection does not induce these structures in infected $CD4^+$ T cells, but their existing TNTs support the direct transfer of HIV-1 to uninfected T cells over long distances (16). DC can act as a ‘Trojan horse’ by sequestering intact HIV-1 virions and mediating *trans*-infection of $CD4^+$ T cells by transmitting virions across the virologic synapse (40). In this report, we demonstrate that HIV-1-like particles can be directly transferred from DC to DC via CD40L-induced TNT networks. In addition to providing a direct conduit for HIV-1 dissemination from migratory DC to susceptible T cells, reticulation may facilitate viral spread from migratory to lymph node resident DC, greatly amplifying the proportion of cells harboring and able to transmit the virus. Interestingly, we have recently shown that HIV-1 can selectively utilize CTL helper activity in the absence of killing as a means to induce and program DC1 capable of efficiently mediating HIV-1 *trans*–infection of $CD4^+$ T cells (26). Although this study shows that such

$CD8^+$ T cell-matured DC1 reticulate in response to CD40L, questions remain regarding the role of reticulation in the scenario of *trans*-infection, and the exact mechanism involved in HIV-1 transfer during natural infection.

DC reticulation may help or harm depending on the context in which it is induced, yet this phenomenon likely represents a fundamental aspect of DC effector function. The increased surface area and spatial reach afforded by this dynamic process can enhance not only the ability of IFN-γ-polarized DC1 to directly transfer activation signals or Ags to other DC subsets, but can also provide DC a greater opportunity to encounter rare cognate T cells for the efficient initiation of adaptive immune responses. While elevated IL-12p70 production in part explains why DC1 are highly effective inducers of $CD8^+$ T cell responses (7, 24), their ability to reticulate and maximize opportunities for critical contact with T cells as well as exchange Ags between interconnected DC are also likely contributing factors.

In addition to demonstrating that pre-programmed DC1 respond to CD40L by forming TNT networks, we show that CD40L and the cytokine IFN-γ can co-stimulate reticulation in mature, non-polarized DC0. These data collectively provide support for the existence of a positive feedback loop whereby successful DC1-driven IFN-γ responses from Th1, CTL, and/or NK cell immune effectors in turn promote continued DC1 polarization (41), and therefore reticulation. Conversely, exposure of DC to the chronic inflammatory mediator PGE_2 during early stages of maturation generates DC2 that not only have a diminished capacity to produce IL-12p70 and promote type-1 immunity (7, 10, 42), but also fail to reticulate in response to CD40 ligation. Furthermore, the Th2 cell-associated cytokine IL-4 substantially inhibits this CD40L-induced process in both DC0 and DC1, suggesting a Th2-driven negative feedback mechanism for inhibiting the reticulation process. Although further study is required to fully understand the regulation and immunologic activity of DC reticulation in vivo, these findings advance our basic comprehension of the mechanisms by which DC bridge innate and adaptive immunity. These results also have important implications in the ongoing quest for therapies to combat cancer and viral pathogens such as HIV-1.

Supplementary Material

Refer to Web version on PubMed Central for supplementary material.

Acknowledgments

The authors thank Greg Gibson, Blair Erdeljac, Diana Campbell, and Angela Anthony for technical assistance, and Drs. Simon Barratt-Boyes and Donna B. Stolz for helpful discussions.

Work supported by National Institute of Allergy and Infectious Diseases Grants U01 AI-35041, R37 AI-41870, and T32 AI-065380

Glossary

DC	dendritic cells
DC1	type-1 polarized DC

DC2	type-2 polarized DC
TNTs	tunneling nanotubes
iDC	immature DC
cIMDM	IMDM supplemented with 10% fetal bovine serum
poly(I:C)	polyisosinic:polycytidylic acid
SEB	staphylococcal enterotoxin B
rh	recombinant human CD40L
J558-CD40L	CD40L-expressing J558 cells
EEA1	early endosomal Ag 1
DIC	differential interference contrast
NA	numerical aperture
VZV	varicella zoster virus
TT	tetanus toxoid
YG	yellow-green
Cy	cyanine dye 5
SFU	spot forming units
FPS	frames per second

References

1. Steinman RM, Banchereau J. Taking dendritic cells into medicine. Nature. 2007; 449:419–426. [PubMed: 17898760]
2. Kalinski P, Hilkens CM, Wierenga EA, Kapsenberg ML. T-cell priming by type-1 and type-2 polarized dendritic cells: the concept of a third signal. Immunology today. 1999; 20:561–567. [PubMed: 10562707]
3. Kapsenberg ML. Dendritic-cell control of pathogen-driven T-cell polarization. Nature reviews. Immunology. 2003; 3:984–993.
4. Bennett SR, Carbone FR, Karamalis F, Flavell RA, Miller JF, Heath WR. Help for cytotoxic-T-cell responses is mediated by CD40 signalling. Nature. 1998; 393:478–480. [PubMed: 9624004]
5. Schoenberger SP, Toes RE, van der Voort EI, Offringa R, Melief CJ. T-cell help for cytotoxic T lymphocytes is mediated by CD40-CD40L interactions. Nature. 1998; 393:480–483. [PubMed: 9624005]
6. Ridge JP, Di Rosa F, Matzinger P. A conditioned dendritic cell can be a temporal bridge between a CD4+ T-helper and a T-killer cell. Nature. 1998; 393:474–478. [PubMed: 9624003]
7. Mailliard RB, Wankowicz-Kalinska A, Cai Q, Wesa A, Hilkens CM, Kapsenberg ML, Kirkwood JM, Storkus WJ, Kalinski P. alpha-type-1 polarized dendritic cells: a novel immunization tool with optimized CTL-inducing activity. Cancer research. 2004; 64:5934–5937. [PubMed: 15342370]
8. Mailliard RB, Son YI, Redlinger R, Coates PT, Giermasz A, Morel PA, Storkus WJ, Kalinski P. Dendritic cells mediate NK cell help for Th1 and CTL responses: two-signal requirement for the induction of NK cell helper function. J Immunol. 2003; 171:2366–2373. [PubMed: 12928383]
9. Trinchieri G. Interleukin-12 and the regulation of innate resistance and adaptive immunity. Nature reviews. Immunology. 2003; 3:133–146.

10. Vieira PL, de Jong EC, Wierenga EA, Kapsenberg ML, Kalinski P. Development of Th1-inducing capacity in myeloid dendritic cells requires environmental instruction. J Immunol. 2000; 164:4507–4512. [PubMed: 10779751]
11. Jongbloed SL, Kassianos AJ, McDonald KJ, Clark GJ, Ju X, Angel CE, Chen CJ, Dunbar PR, Wadley RB, Jeet V, Vulink AJ, Hart DN, Radford KJ. Human CD141+ (BDCA-3)+ dendritic cells (DCs) represent a unique myeloid DC subset that cross-presents necrotic cell antigens. The Journal of experimental medicine. 2010; 207:1247–1260. [PubMed: 20479116]
12. Allan RS, Waithman J, Bedoui S, Jones CM, Villadangos JA, Zhan Y, Lew AM, Shortman K, Heath WR, Carbone FR. Migratory dendritic cells transfer antigen to a lymph node-resident dendritic cell population for efficient CTL priming. Immunity. 2006; 25:153–162. [PubMed: 16860764]
13. Qu C, Nguyen VA, Merad M, Randolph GJ. MHC class I/peptide transfer between dendritic cells overcomes poor cross-presentation by monocyte-derived APCs that engulf dying cells. J Immunol. 2009; 182:3650–3659. [PubMed: 19265143]
14. Bousso P. T-cell activation by dendritic cells in the lymph node: lessons from the movies. Nature reviews. Immunology. 2008; 8:675–684.
15. Rustom A, Saffrich R, Markovic I, Walther P, Gerdes HH. Nanotubular highways for intercellular organelle transport. Science. 2004; 303:1007–1010. [PubMed: 14963329]
16. Davis DM, Sowinski S. Membrane nanotubes: dynamic long-distance connections between animal cells. Nature reviews. Molecular cell biology. 2008; 9:431–436.
17. Watkins SC, Salter RD. Functional connectivity between immune cells mediated by tunneling nanotubules. Immunity. 2005; 23:309–318. [PubMed: 16169503]
18. Snijders A, Kalinski P, Hilkens CM, Kapsenberg ML. High-level IL-12 production by human dendritic cells requires two signals. International immunology. 1998; 10:1593–1598. [PubMed: 9846688]
19. Mailliard RB, Egawa S, Cai Q, Kalinska A, Bykovskaya SN, Lotze MT, Kapsenberg ML, Storkus WJ, Kalinski P. Complementary dendritic cell-activating function of CD8+ and CD4+ T cells: helper role of CD8+ T cells in the development of T helper type 1 responses. The Journal of experimental medicine. 2002; 195:473–483. [PubMed: 11854360]
20. Onfelt B, Nedvetzki S, Yanagi K, Davis DM. Cutting edge: Membrane nanotubes connect immune cells. J Immunol. 2004; 173:1511–1513. [PubMed: 15265877]
21. Nielsen JS, Wick DA, Tran E, Nelson BH, Webb JR. An in vitro-transcribed-mRNA polyepitope construct encoding 32 distinct HLA class I-restricted epitopes from CMV, EBV, and Influenza for use as a functional control in human immune monitoring studies. Journal of immunological methods. 2010; 360:149–156. [PubMed: 20637775]
22. Keating SM, Bejon P, Berthoud T, Vuola JM, Todryk S, Webster DP, Dunachie SJ, Moorthy VS, McConkey SJ, Gilbert SC, Hill AV. Durable human memory T cells quantifiable by cultured enzyme-linked immunospot assays are induced by heterologous prime boost immunization and correlate with protection against malaria. J Immunol. 2005; 175:5675–5680. [PubMed: 16237057]
23. Pan J, Zhang M, Wang J, Wang Q, Xia D, Sun W, Zhang L, Yu H, Liu Y, Cao X. Interferon-gamma is an autocrine mediator for dendritic cell maturation. Immunology letters. 2004; 94:141–151. [PubMed: 15234546]
24. Ten Brinke A, Karsten ML, Dieker MC, Zwaginga JJ, van Ham SM. The clinical grade maturation cocktail monophosphoryl lipid A plus IFNgamma generates monocyte-derived dendritic cells with the capacity to migrate and induce Th1 polarization. Vaccine. 2007; 25:7145–7152. [PubMed: 17719152]
25. Napolitani G, Rinaldi A, Bertoni F, Sallusto F, Lanzavecchia A. Selected Toll-like receptor agonist combinations synergistically trigger a T helper type 1-polarizing program in dendritic cells. Nature immunology. 2005; 6:769–776. [PubMed: 15995707]
26. Mailliard RB, Smith KN, Fecek RJ, Rappocciolo G, Nascimento EJ, Marques ET, Watkins SC, Mullins JI, Rinaldo CR. Selective Induction of CTL Helper Rather Than Killer Activity by Natural Epitope Variants Promotes Dendritic Cell-Mediated HIV-1 Dissemination. J Immunol. 2013; 191:2570–2580. [PubMed: 23913962]

27. Cheong C, Matos I, Choi JH, Dandamudi DB, Shrestha E, Longhi MP, Jeffrey KL, Anthony RM, Kluger C, Nchinda G, Koh H, Rodriguez A, Idoyaga J, Pack M, Velinzon K, Park CG, Steinman RM. Microbial stimulation fully differentiates monocytes to DC-SIGN/CD209(+) dendritic cells for immune T cell areas. Cell. 2010; 143:416–429. [PubMed: 21029863]
28. Schiller C, Huber JE, Diakopoulos KN, Weiss EH. Tunneling nanotubes enable intercellular transfer of MHC class I molecules. Human immunology. 2013; 74:412–416. [PubMed: 23228397]
29. Onfelt B, Nedvetzki S, Benninger RK, Purbhoo MA, Sowinski S, Hume AN, Seabra MC, Neil MA, French PM, Davis DM. Structurally distinct membrane nanotubes between human macrophages support long-distance vesicular traffic or surfing of bacteria. J Immunol. 2006; 177:8476–8483. [PubMed: 17142745]
30. Eugenin EA, Gaskill PJ, Berman JW. Tunneling nanotubes (TNT) are induced by HIV-infection of macrophages: a potential mechanism for intercellular HIV trafficking. Cellular immunology. 2009; 254:142–148. [PubMed: 18835599]
31. Kadiu I, Gendelman HE. Human immunodeficiency virus type 1 endocytic trafficking through macrophage bridging conduits facilitates spread of infection. Journal of neuroimmune pharmacology : the official journal of the Society on NeuroImmune Pharmacology. 2011; 6:658–675. [PubMed: 21789505]
32. Chinnery HR, Pearlman E, McMenamin PG. Cutting edge: Membrane nanotubes in vivo: a feature of MHC class II+ cells in the mouse cornea. J Immunol. 2008; 180:5779–5783. [PubMed: 18424694]
33. Albert ML, Sauter B, Bhardwaj N. Dendritic cells acquire antigen from apoptotic cells and induce class I-restricted CTLs. Nature. 1998; 392:86–89. [PubMed: 9510252]
34. Andre F, Chaput N, Schartz NE, Flament C, Aubert N, Bernard J, Lemonnier F, Raposo G, Escudier B, Hsu DH, Tursz T, Amigorena S, Angevin E, Zitvogel L. Exosomes as potent cell-free peptide-based vaccine. I. Dendritic cell-derived exosomes transfer functional MHC class I/peptide complexes to dendritic cells. J Immunol. 2004; 172:2126–2136. [PubMed: 14764678]
35. Harshyne LA, Watkins SC, Gambotto A, Barratt-Boyes SM. Dendritic cells acquire antigens from live cells for cross-presentation to CTL. J Immunol. 2001; 166:3717–3723. [PubMed: 11238612]
36. Kastenmuller W, Gerner MY, Germain RN. The in situ dynamics of dendritic cell interactions. European journal of immunology. 2010; 40:2103–2106. [PubMed: 20853494]
37. Lindquist RL, Shakhar G, Dudziak D, Wardemann H, Eisenreich T, Dustin ML, Nussenzweig MC. Visualizing dendritic cell networks in vivo. Nature immunology. 2004; 5:1243–1250. [PubMed: 15543150]
38. Chieppa M, Rescigno M, Huang AY, Germain RN. Dynamic imaging of dendritic cell extension into the small bowel lumen in response to epithelial cell TLR engagement. The Journal of experimental medicine. 2006; 203:2841–2852. [PubMed: 17145958]
39. Lou E, Fujisawa S, Morozov A, Barlas A, Romin Y, Dogan Y, Gholami S, Moreira AL, Manova-Todorova K, Moore MA. Tunneling nanotubes provide a unique conduit for intercellular transfer of cellular contents in human malignant pleural mesothelioma. PloS one. 2012; 7:e33093. [PubMed: 22427958]
40. Rinaldo CR. HIV-1 Trans Infection of CD4(+) T Cells by Professional Antigen Presenting Cells. Scientifica (Cairo). 2013; 2013:164–203.
41. Kalinski P, Moser M. Consensual immunity: success-driven development of T-helper-1 and T-helper-2 responses. Nature reviews. Immunology. 2005; 5:251–260.
42. Kalinski P. Regulation of immune responses by prostaglandin E2. J Immunol. 2012; 188:21–28. [PubMed: 22187483]

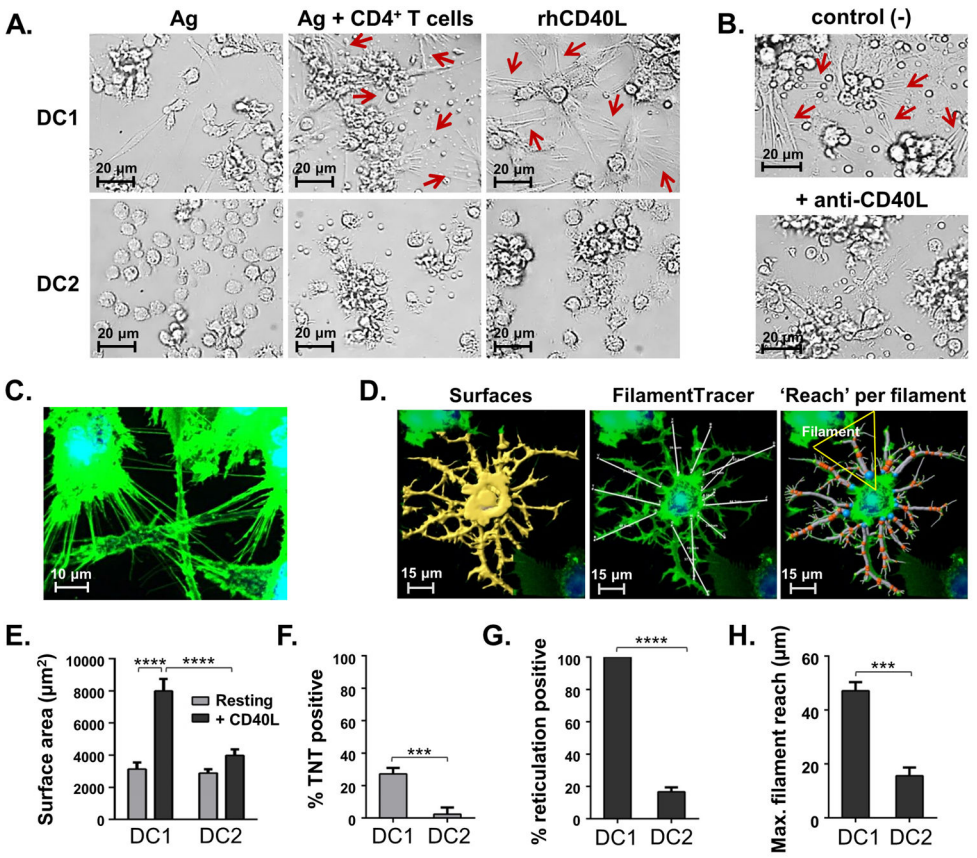

Figure 1. CD4$^+$ Th cell-associated CD40L induces TNT-like protrusions that greatly increase the surface area and spatial reach of individual DC1

(**A**) Bright field images (400×) of mature DC1 or DC2 co-cultured in the presence of SEB alone (left panels) or with CD4$^+$ T cells (middle panels), or rhCD40L (right panels) for 24 h. The arrows highlight TNT-like extensions. (**B**) 24 h co-cultures of SEB Ag-presenting DC1 and CD4$^+$ T cells in the presence of control mAb (top) or CD40L blocking mAb (bottom). (**C**) Representative Z-series projection image revealing a network of TNT-like membrane connections in fluorescently labeled DC1. (A-C) Images are representative of 6 independent experiments conducted on DC from 3 healthy donors. (**D**) Representative Z-series projection images of a CD40L-activated DC1 analyzed using the IMARIS 'Surfaces' program to determine total cell surface area (left panel), and IMARIS 'FilamentTracer' to trace the pathway of each 'filament' branch extending from a single origin (blue sphere) at the edge of the cell body (middle panel). Individual segments begin at an origin or branch point (orange spheres) and end at the next branch or terminal point (green spheres). Spatial 'reach' was defined as the shortest distance from a filament origin to the distal terminal point of that filament (right panel; white lines connecting 2 points). (**E**) Total cell surface area comparisons of resting and CD40L-activated DC1 and DC2. (**F**) Comparison of percentage 'TNT positive' resting DC1 and DC2 (media only), defined as those expressing ≥5 individual TNTs per cell that were each >5.0 μm in length. (**G**) Comparison of percentage 'reticulation positive' CD40L-activated DC1 and DC2, delineated as those displaying ≥5 filaments per cell that were each >10.0 μm in sum segment length. (**H**) 'Maximum reach' of

filaments, defined as the shortest distance (μm) from the origin to the farthest terminal point of a filament. (E-H) Data were generated from randomly chosen image fields (20–30 per donor) and represented as mean ± SD of 3 healthy donors independently tested. P-values <0.0001, <0.001, <0.01 and <0.05 are represented by ****, ***, **, and *, respectively. See also Supplemental Fig. 1; Video 1; Video 2.

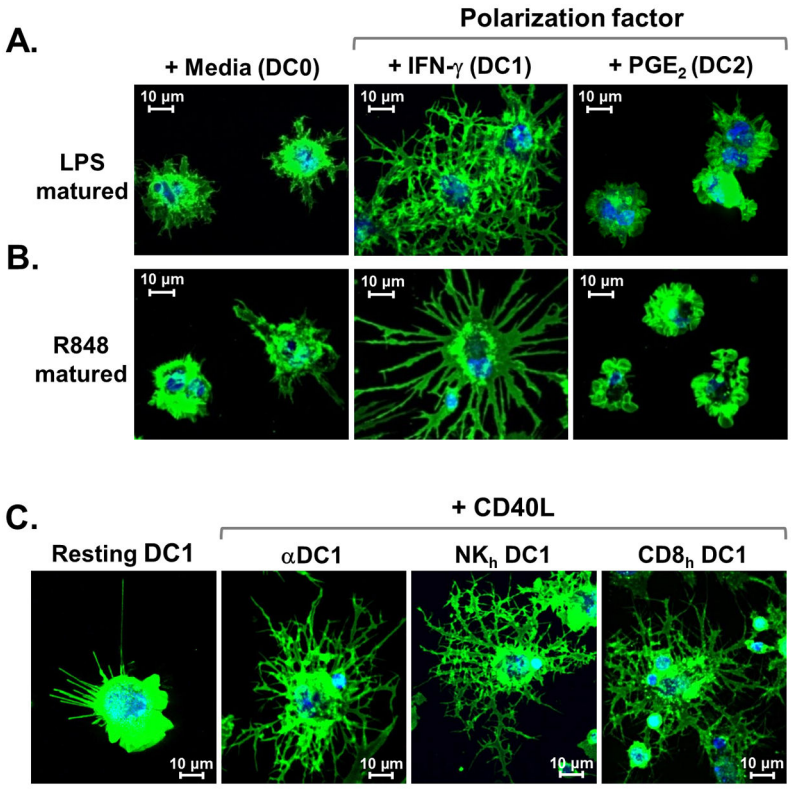

Figure 2. Reticulation in response to CD40L is a trait of DC matured in the presence of type-1 inflammatory mediators

(**A–C**) 3D reconstruction images (600×) of differentially matured DC stimulated for 20 h with rhCD40L prior to labeling the cell surface with MHC class I mAb (green) and labeling nuclei (blue), followed by live-cell confocal imaging. Data are representative of 6 independent experiments conducted using DC from 3 healthy donors. (**A**) Membrane morphologies of mature CD40L-activated DC0, DC1, and DC2 propagated using LPS alone, LPS + IFN-γ, or LPS + PGE_2, respectively. (**B**) Mature CD40L-treated DC0, DC1, and DC2 generated by the respective use of R848 alone, R848 + IFN-γ, or R848 + PGE_2. (**C**) Cell morphologies of DC1 treated with media alone or CD40L. DC1 were generated using the αDC1 cytokine-based cocktail (first two panels on left), or induced by 48 h co-culture of iDC with either 2-signal activated NK_h cells (middle) or SEB-activated $CD8^+$ T cells (right).

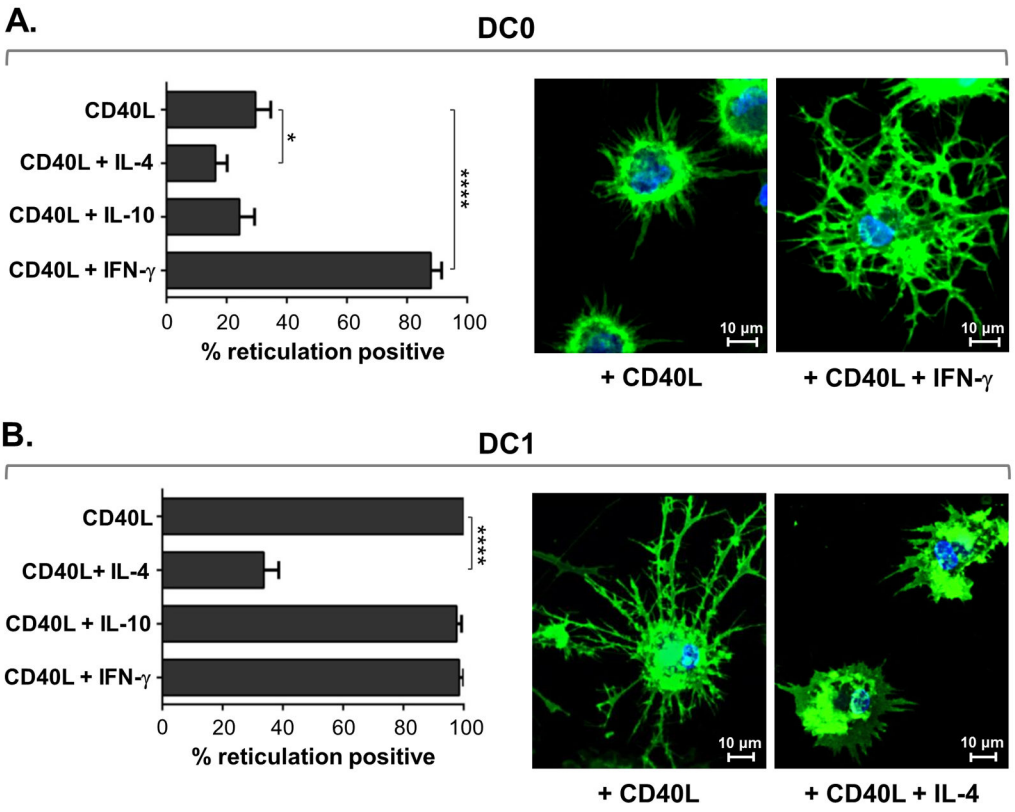

Figure 3. DC reticulation is enhanced by the Th1 cytokine IFN-γ, and inhibited by the Th2 cytokine IL-4

(**A**) Graphical display of the percentage of reticulation positive TNF-α-matured DC0 after 20 h exposure to rhCD40L alone, or in combination with IL-4, IL-10, or IFN-γ. Also shown are representative confocal images (600×) of DC0 stimulated with rhCD40L alone or in combination with IFN-γ and then surface labeled with MHC class I-specific mAb (green) and nuclear labeled (blue). (**B**) Graphical depiction of percentage reticulation positive αDC1 after 20 h exposure to rhCD40L alone, or combined with IL-4, IL-10, or IFN-γ. Additionally shown are representative confocal images (600×) of DC1 stimulated with rhCD40L alone or in combination with IL-4. (A-B) Quantitative data, displayed as percentage positive ± SE, are representative of 3 healthy donors independently tested twice per donor. See also Supplemental Fig. 2.

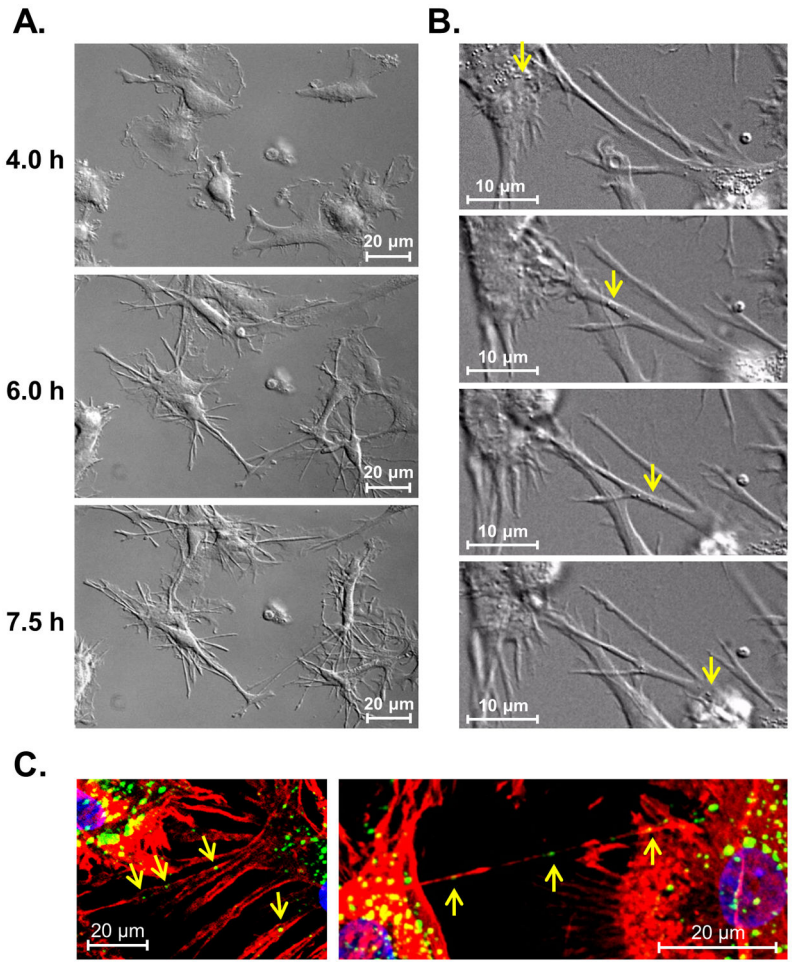

Figure 4. CD40L-induced reticulation supports intercellular trafficking of endogenous cell structures between DC

(**A**) Sequential still frames of DC1 actively reticulating from 4 to 7.6 h post-addition of rhCD40L, captured by live-cell, time-lapse DIC imaging (600×). See also Video 3. (**B**) Sequential frames of high resolution, time-lapse DIC imaging (600×) of live 8 h rhCD40L-stimulated DC1 showing endogenous cell structures resembling vesicles (arrows) trafficking between neighboring cells through CD40L-induced TNTs. See also Video 4. (**C**) Confocal reconstruction images (1000×) revealing early endosome- (green, arrows) and F-actin-containing TNTs (red) and nuclei (blue) in fixed CD40L-activated DC1. Data are representative of 3 donors independently tested.

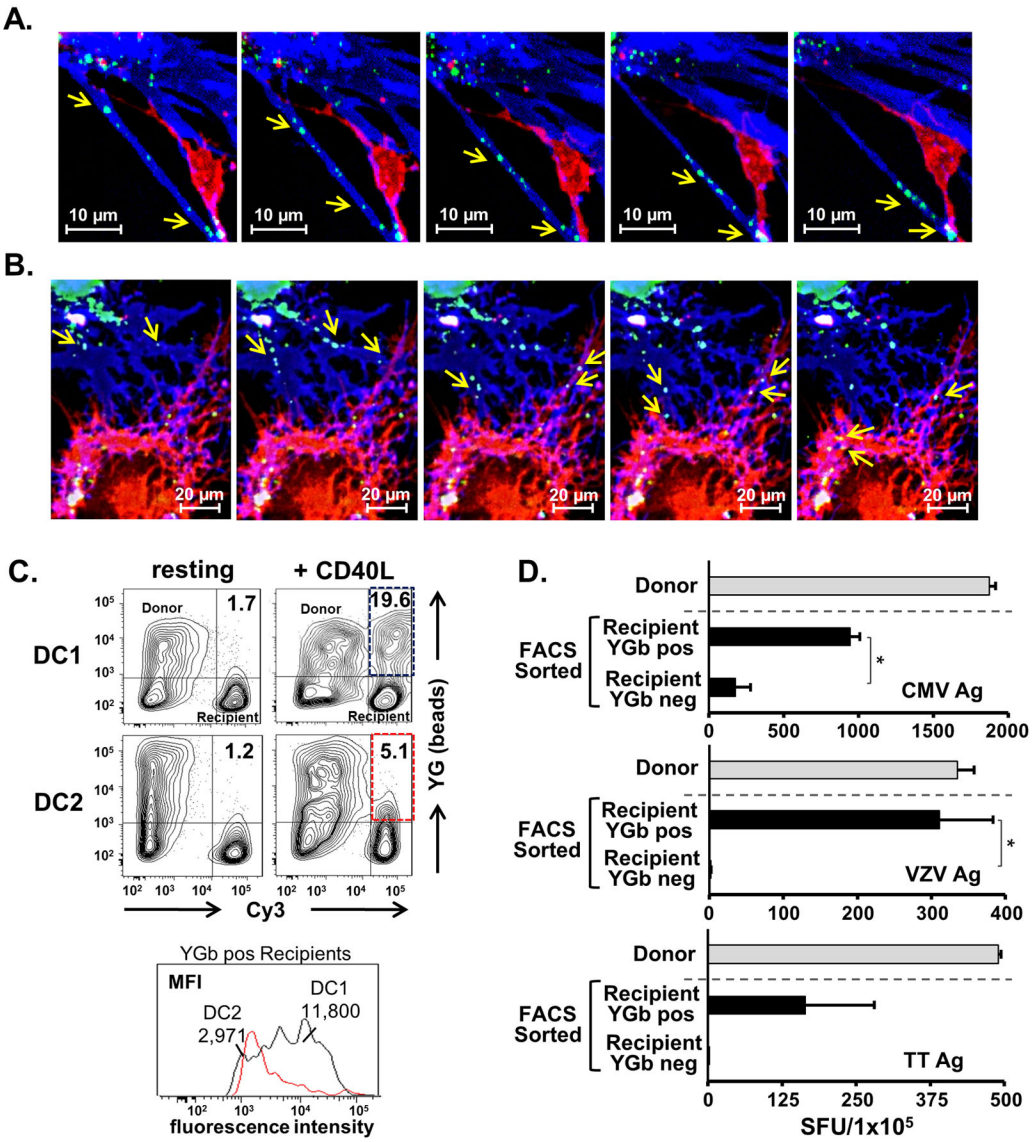

Figure 5. CD40L-induced reticulation facilitates the intercellular transfer of exogenous Ag between DC1

(**A–C**) Cy5-labeled (blue), YG latex bead (40 nm)-containing ‘donor’ DC1 or DC2 were co-cultured with the respective non-bead-containing, Cy3-labeled (red) ‘recipient’ DC type for 20 h in the presence or absence of rhCD40L. Data are representative of 2 donors independently tested. (**A**) Montage of time-lapse, confocal imaging (600×) showing beads (green; arrows) moving rapidly through donor DC1 TNTs (blue) over a time span of 28 min. See also Video 5. (**B**) Montage tracing the pathway of beads (green; arrows) traveling from the cell body of donor DC1 (blue), through donor cell TNTs and into the connected recipient DC (red), where they finally collect in the recipient cell body (yellow, lower left arrows). (**C**) Flow cytometric analysis and quantification of intercellular exogenous bead transfer from donor to recipient DC types after treatment with media only or CD40L. (**D**) IFNγ-ELISPOT assays measuring Ag-specific recall responses of cultured T cells following their in vitro sensitization with FACS sorted, YG bead/Ag positive and negative recipient DC1.

Data are represented as mean ± SE of 2 independent experiments, and * represents the p-value <0.05. See also Supplemental Fig. 3.

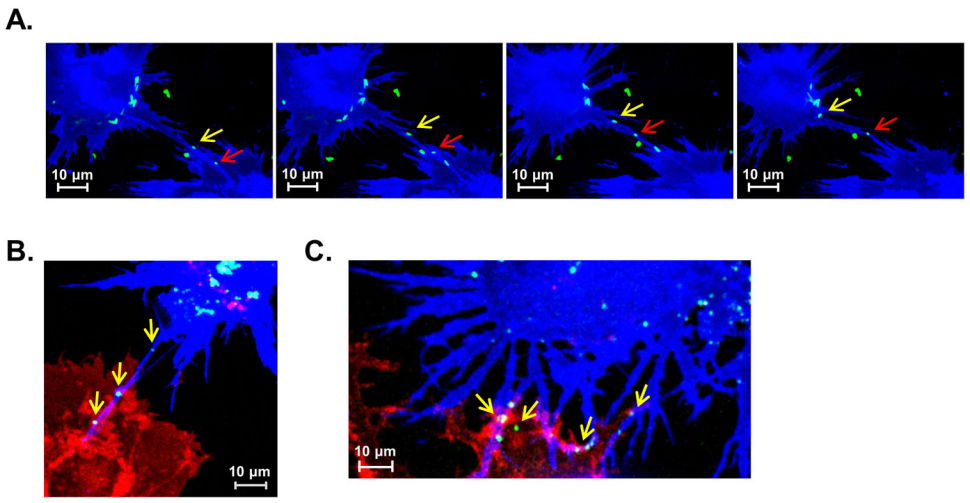

Figure 6. Pathogens can utilize CD40L-induced TNT networks for direct cell-to-cell spread

(**A**) DC1 monolayers that had been stimulated with rhCD40L for 10 h were exposed to EGFP-expressing *Escherichia coli* for 2 h. Subsequent time-lapse confocal resonant scanning microscopy shows individual bacterium (green) trafficking bi-directionally along CD40L-induced TNTs (arrows) between mature DC1. See also Video 6. (**B**) Donor DC1 (blue) pulsed with EGFP-expressing HIV-1-like particles (green) were co-cultured with recipient DC1 (red) in the presence of CD40L for 10 h prior to live-cell imaging. HIV-1-like particles localizing to a donor cell nanotube (blue; arrows) that has formed a connection with a recipient cell body. (**C**) At 20 h post-CD40L stimulation, HIV-1-like particles can be detected at the interface between blue donor cell TNTs and red recipient cells (arrows), prior to their subsequent transfer to recipient cell bodies. (A-C) Imaging data are representative of 3 donors independently tested.